THE PARADISO CAMPAIGN: DESCRIPTION AND FIRST RESULTS

Jordi Figueras i Ventura[1]*, Marc Schneebeli[1], Andreas Leuenberger[1], Marco Gabella[1],
Jacopo Grazioli[2], Timothy Hugh Raupach[2], Daniel Wolfensberger[2], Pascal Graf[3], Heini Wernli[3],
Alexis Berne[2] and Urs Germann[1]
[1]MeteoSwiss, Locarno, Switzerland
[2]EPFL, Lausanne, Switzerland
[3]ETH Zurich, Zurich, Switzerland

1. INTRODUCTION

The PARADISO campaign (PAyerne Radar Disdrometer and ISOtope) was a joint venture between the Environmental Remote Sensing Laboratory (LTE) of the Swiss Federal Institute of Technology in Lausanne (EPFL), the Atmospheric Dynamics group of the Institute for Atmospheric and Climate Science of the Swiss Federal Institute of Technology in Zurich (ETHZ) and the Radar, Satellite and Nowcasting and Atmospheric Data Divisions of MeteoSwiss, with the logistical support of the MeteoSwiss headquarters at Payerne.

The main objectives of the campaign were firstly to investigate aspects of the microphysics of clouds and precipitation and the atmosphere dynamics and secondly to validate and improve several remote sensing calibration and retrieval techniques. The measurement period took place between end of March and beginning of July 2014 in the area surrounding Payerne, in the Swiss plateau.

This paper describes the instrument setup, discusses the data availability and quality and highlights some of the results regarding remote sensing retrieval techniques.
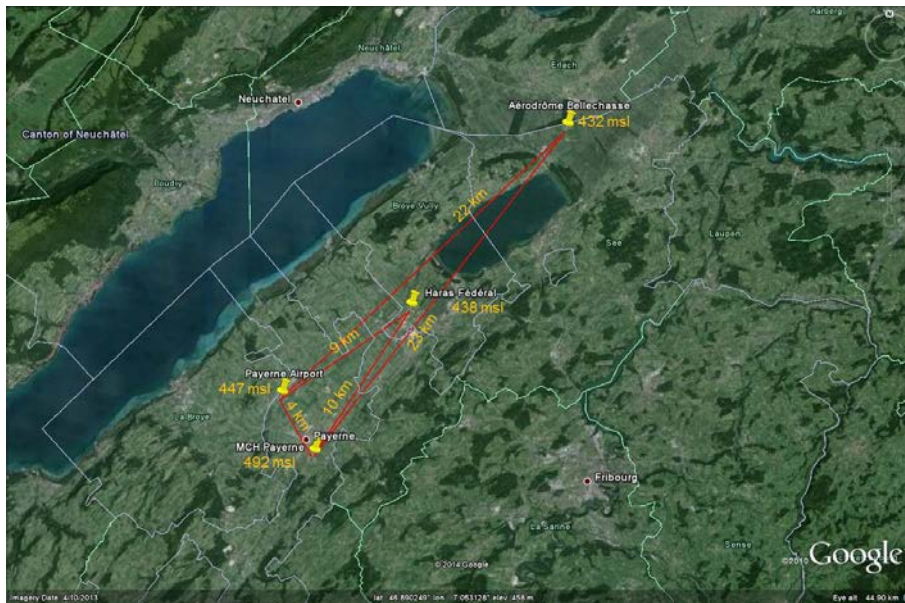
Fig. 1 Instrumented sites

2. INSTRUMENT SETUP AND DATA AVAILABILITY

Several instruments were deployed specifically for the campaign: 2 X-band Doppler polarimetric weather radars (Meteor 50DX, in the following called DX50, from SELEX ES and operated by MeteoSwiss and MXPol from ProSensing and operated by EPFL), a mobile wind profiler, 5 Parsivel disdrometers (1st generation), a 2D video disdrometer and a Picarro water vapor isotope analyzer. In addition to that, operational models and data from MeteoSwiss, such as data from the weather stations of the SwissMetNet network, the operational radio sounding at Payerne, the C-band weather radar network and the COSMO numerical weather prediction (NWP) model were collected.

---

* *Corresponding author address:* Jordi Figueras i Ventura, MeteoSwiss, Switzerland, +41 917562306; e-mail: jordi.figuerasiventura@meteoswiss.ch.

The instruments were deployed at 4 different measurement sites (See Fig. 1). The DX50 and one Parsivel disdrometer were set up at the Payerne military airport, the MXPol, 2 Parsivel disdrometers , the video disdrometer and the isotope analyzer were set up at the MeteoSwiss headquarters in Payerne, 4 km southeast of the airport. Another instrumented site, with the wind profiler and one disdrometer, was placed 9 km northeast at Avenches. Finally a disdrometer was set 22 km northeast of the Payerne airport, at Bellechasse, almost aligned with the instruments at Avenches. In this way a transect of 3 measurement locations, from southwest to northeast, allowed to monitor the typical flow of precipitating systems in the plateau. In addition to the deployed instruments, data from weather stations at Mathod and Neuchâtel and the La Dôle operational C-band radar (80 km south east of the area of interest) were collected.

The scanning strategy of the DX50 consisted of 3 RHIs by the instrumented sites, 3 PPIs at elevations 4, 6 and 25° and a vertically pointing scan, meant for the retrieval of drop size distribution (DSD) and differential reflectivity Z_{dr} calibration, which were repeated every 5 minutes. During the RHIs and the vertically pointing scan, the Doppler spectra were recorded.

The scanning strategy of the MXPOL consisted of 2 RHIs, one in the direction of the DX50 and the other roughly in the direction of the two other instrumented sites, a PPI at 5° and a vertically pointing scanning. The repetition time was also 5 minutes.

The scans were synchronized so that when one radar was performing the vertically pointing scan the other radar was performing the RHI over the radar site. The two radars would also simultaneously perform the RHI scans over the other 2 instrumented sites and the set of PPIs. This facilitates the inter-comparison of the data and allows the study of attenuation effects since both radars were measuring at the same instrumented sites from slightly different angles.

The water vapor isotope analyzer continuously collected data from 21 March to 16 June 2014. In addition, sequential precipitation samples with 10 minutes resolution were manually collected at the MeteoSwiss headquarters in Payerne during rain events on 22 March, 22 May and 4 June. The isotopic composition of these rain samples was later analysed in the lab, also using a Picarro laser-based spectrometer.

DX50 radar data was collected on a continuous basis from 21 March to 4 July 2014 except for a period between 3 to 26 June where the radar was not working due to a failure in the magnetron. The MXPol collected data from 21

March to 19 May with several interruptions due to hardware problems. A total of 26 days with significant rainfall, of which 10 were observed simultaneously by both radars, were recorded.

3. DATA QUALITY

Data quality of the polarimetric moments Z_{dr}, co-polar correlation coefficient ρ_{hv} and differential phase Φ_{dp} offset was monitored following similar techniques to those described in Figueras i Ventura et al. (2012) while the horizontal reflectivity Z_h calibration was monitored using the self-consistency principle described in Gourley et al. (2009). In addition the reflectivity of the DX50, MXPol and La Dôle radars was inter-compared using the method described in Figueras i Ventura et al (2013).

a)

b)
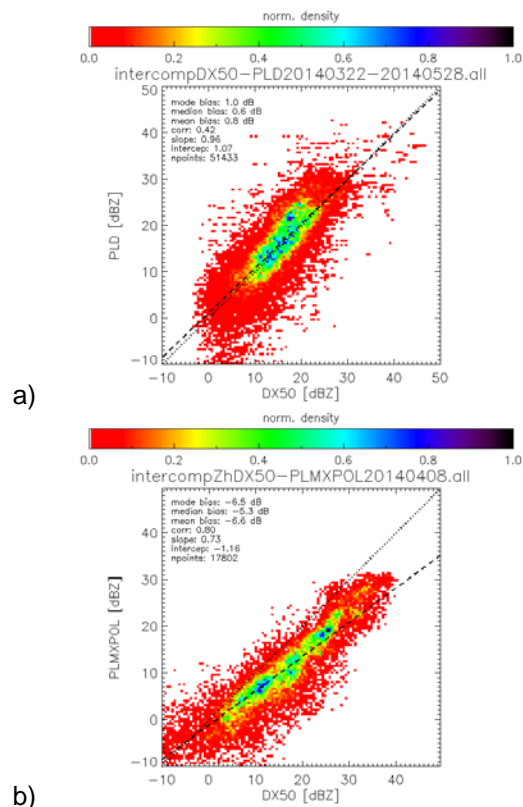
Fig. 2 Z_h inter-comparison between: a) DX50 and La Dole radars for the first part of the campaign, b) DX50 and MXPol radars for day 2014-04-08

The results for the DX50 were the following: Φ_{dp} offset was stable during the entire campaign with values in the order of -147° for the first part of the campaign (before the magnetron failed) and -162° during the second part of the campaign. Z_{dr} bias was on the order of 0.2 dB during the entire campaign except for a transitional period at the beginning of the second part of the campaign where the bias was as high as 0.8 dB. ρ_{hv} in rain was relatively low, but generally speaking well above 0.98. Z_h bias was

on the order of 2 to 3 dB. However, this bias includes the effect of radome attenuation and under-correction of precipitation-induced path attenuation. When comparing the DX50 reflectivity with that of La Dôle the median bias was below 1 dB (See Fig. 2a).

An overall analysis of the performance of the MXPol has yet to be performed. However the analysis of the data on 8 April 2014 shows that the Φ_{dp} offset was 20°, the Z_{dr} bias on the order of -0.1 dB and the ρ_{hv} was much higher than the DX50, 0.996. Z_h according to self-consistency had a bias of -5 dB. This is in line with the comparison with the DX50 that also points to a bias of -5 dB in reflectivity (See Fig. 2b). It should be noticed that right after this event the magnetron failed so the large bias it is likely linked to poor performance of the magnetron.

4. PRELIMINARY RESULTS

4.1 *Wind Profiling*

The radial wind retrieved by the DX50 above the location of the wind profiler was compared with the profiler data. To do so, the wind vector measured by the wind profiler was projected to the radial direction from the weather radar while the radar wind samples where averaged to the same time period of the wind profiler (20 min). Two scores were computed: the absolute difference between the wind profiler data and the radar data and the relative difference respect to the wind profiler.

The comparison showed that the absolute difference between the 2 instruments was less than 2 m/s, while the relative difference was less than 10% most of the time. This is remarkable considering that the different nature of the measurements. In few cases, large relative differences (above 40%) occurred when the wind velocity was very small there were few radar samples due to intermittent precipitation within the integration time.

4.2 *Quantitative Precipitation Estimation*

Six quantitative precipitation estimation algorithms were examined: 1) a simple Z_h-R relation, 2) the same Z_h-R relation but with the reflectivity corrected for attenuation, 3) a K_{dp}-R relation, 4) a relation between specific attenuation and rainfall, A_h-R, following a similar method to Ryzhkov et al. (2014), 5) a combination of Z_h-R relations in which the coefficients are a function of the position respect to the melting layer (below, within or above), 6) same as 5) but using a combination of Z_h-R and A_h-R below the melting layer.

The melting layer was estimated using an adaptation of the algorithm by Giangrande et al.

(2008) which shows a very good agreement with the position of the iso-0° height (See Fig. 3).
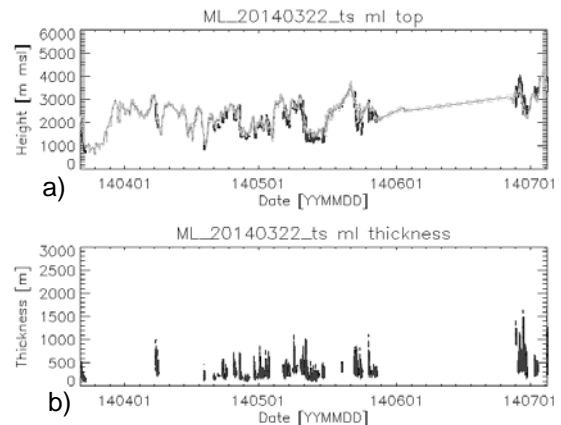
Fig. 3 a) Grey line: altitude of the iso-0° according to COSMO NWP model, black line: Position of the melting layer top. b) Melting layer thickness

To assess the performance of the different algorithms, the lowest elevation available over the two rain gauges and two disdrometers in the vicinity of the DX50 were used. The hourly rainfall accumulation of the different sensors was computed. Three scores were computed, the normalized bias, the correlation and the root mean square error. A summary of the scores can be seen in table 1.

Table 1 Score of the tested QPE algorithms

Algorithm	NP	NB	corr	RMS [mm]
R-Zh no att corr	976	-0.29	0.73	0.84
R-Kdp	727	2.00	0.53	2.67
R-Ah	637	0.79	0.79	1.16
R-Zh	940	-0.14	0.73	0.83
R-ML	940	-0.15	0.79	0.74
R-ML2	940	0.07	0.80	0.75

The simple Z_h-R relationship exhibited a substantial underestimation of precipitation (NB= -0.29) which was partially palliated by the correction of attenuation (NB=-0.14). K_{DP}-R was heavily overestimating precipitation (NB=2.00), particularly for less intense precipitation. The latter is expected since negative rainfall rates were set to 0 mm/h. Also the correlation was rather poor. A_h-R was performing better than K_{DP}-R, which seems to confirm the superiority of A_h with respect to K_{dp} as shown in Diederich et al. (2015). Most likely this is due to the coarser resolution that can be achieved using K_{dp}. Our implementation of A_h-R was substantially overestimating precipitation (NB=0.79). However the correlation was better than that of the Z_h-R based algorithms. The use of different Z_h-R relationships depending on the precipitation phase resulted in similar normalized biases than a single Z_h-R relation but a better correlation and lower RMS. The combination of reflectivity and

specific attenuation-based retrievals in the liquid phase area improved slightly the correlation and resulted in a positive bias of 0.07. Hence, this seems to be the best retrieval of the 6 analyzed.

It should be noticed that since the lowest elevation possible was used for the measurements, a large percentage of the measurements were performed in the liquid phase of precipitation. Only measurements, performed over the rain gauges, that had to use the lowest PPI scan of 4°, were in the melting layer or above. Consequently, one should expect the differences between algorithms to increase if the measurements had to be performed higher up with respect to the ground.

4.3 *Spectral Polarimetry*

The Doppler spectrum has the potential to provide information of the scatterers within a resolution volume since data in the spectrum is clustered in Doppler bins and weather echoes may have different signatures than clutter (see Moisseev and Chandrasekar, 2009). Theoretically it is even possible to retrieve the DSD from the Doppler spectrum (see for example Moisseev and Chandrasekar, 2007).

We compute the spectral moments in order to test the feasibility of performing spectral clutter identification in an operational environment and qualitatively evaluate the polarimetric variables obtained via spectral processing respect to those obtained by time domain processing.

To obtain the Doppler spectrum a discrete Fourier transform is performed over the complex (I and Q) time domain signal having the same pulse repetition frequency (PRF). In our case the spectrum was recorded only for RHI and vertically pointing data.

One of the main problems in computing the Doppler spectrum in relatively fast operational scans is that the influence of noise in the measurements increases due to the lack of independent samples. In order to reduce the noise influence, the average noise power per Doppler bin is computed and a clipping of the Doppler bins that are below 10 dB above noise is performed. Furthermore, a moving Gaussian window spanning 5 Doppler bins is applied in the computation of the spectral power.

The spectral moments, which are analogous to the polarimetric moments in time domain, are then computed as:

$$sZ_h[k] = 10 log_{10}\left(C\left(|V_h[k]|^2 - \frac{N_h}{n_D} \right) \right) \quad (1)$$

$$sZ_{dr}[k] = sZ_h[k] - sZ_v[k] \quad (2)$$

$$s\phi_{dp}[k] = -(\phi_h[k] - \phi_v[k]) \quad (3)$$

$$s\rho_{hv[k]} = \left| \frac{V_h^*[k]V_v[k]}{\sqrt{\left(\frac{P_h - N_h}{n_D}\right)\left(\frac{P_v - N_v}{n_D}\right)}} \right| \quad (4)$$

Where $V_x[k]$ is the Fourier transform of the received signal (h or v channels), Φ_x is the phase of the received signal in the frequency domain, P_x and N_x are the signal and noise power respectively, C is the radar constant and n_D is the number of Doppler bins. Additionally, the texture of sZ_{dr} and $s\Phi_{dp}$ is computed as the local standard deviation over 5 Doppler bins.

In order to suppress non-weather signals, Doppler bins with $s\rho_{hv}$ below 0.1, sZ_{dr} below -5 dB, texture of sZ_{dr} above 10 dB and texture of $s\Phi_{dp}$ above 150° are filtered out. This is arguably a very gentle filtering. An optimization of such threshold has yet to be performed.

The polarimetric moments at each range bin can then be computed from the spectrum as:

$$Z_h = 10 log_{10}\left(\sum_{\forall k \in atm} 10^{\frac{sZ_h[k]}{10}} \right) \quad (5)$$

$$Z_{dr} = Z_h - Z_v \quad (6)$$

$$\phi_{dp} = \frac{\sum_{\forall k \in atm} s\phi_{dp}[k] 10^{\frac{sZ_h[k]}{10}}}{\sum_{\forall k \in atm} 10^{\frac{sZ_h[k]}{10}}} \quad (7)$$

$$\rho_{hv} = \frac{|\sum_{\forall k \in atm} V_h^*[k]V_v[k]|}{\sqrt{(P_h - N_h)(P_v - N_v)}} \quad (8)$$

An example of such processing, compared with the time domain processing, is shown in Fig. 4. It should be noticed that the spectral processing has an (oversampled) angular resolution of 0.5° while the time domain has a resolution of 1°. This is due to the fact that the RHI scan had a staggered pulse repetition time (PRT) and therefore the spectral processing was performed in two blocks of 0.5°. Qualitatively both methods yield similar results. The most striking difference is the large improvement in ρ_{hv} in the spectral processing. This is most likely due to a better filtering and estimation of the noise levels. It can also be seen that Doppler width information has been recovered in areas where the Doppler filter applied in the time domain processing has filtered out completely the data.

5. CONCLUSIONS AND FUTURE WORK

A measurement campaign was performed during the spring and early summer of 2014. Several instruments were deployed, including two X-band Doppler polarimetric radars, several disdrometers and a wind profiler.

A valuable data set was collected. 26 major precipitation events were recorded, of which 10 were observed simultaneously by the two X-

band radars. In terms of data quality, the results have confirmed the long term stability of the DX50. The reflectivity in rain was 2 to 3 dB lower than expected, most likely due to under-correction of the path attenuation and the radome attenuation. ρ_{hv} was significantly lower than expected. However, the comparison between ρ_{hv} obtained from time domain processing respect to the spectral processing shows that this is most likely due to poor signal processing and it is not related to antenna performance. The Z_{dr} bias was in the order of 0.2 dB during the entire campaign. An in-depth analysis of the data quality of the MXPol has yet to be performed but a bias of about 5 dB in reflectivity was measured before a hardware failure. Overall, though, the radar data quality is deemed to be satisfactory.
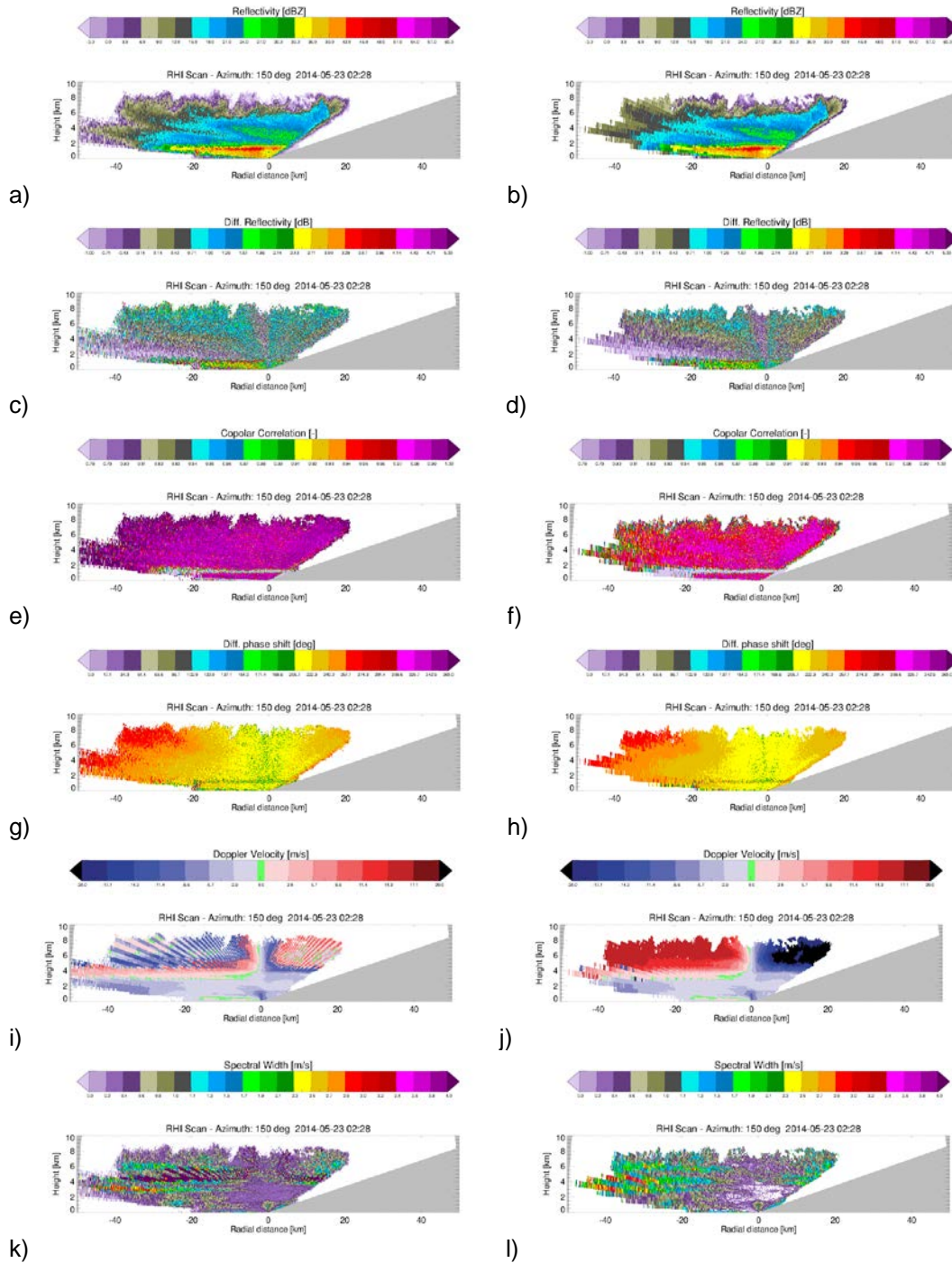
Fig. 4 Example of polarimetric variables obtained from and RHI the 23 May 2014 at 02:28 UTC. Left, spectral processing, right, time domain processing, from top to bottom: Z_h, Z_{dr}, ρ_{hv}, Φ_{dp}, V_D and W_D.

One of the objectives of the campaign was the assessment of the performance of remote sensing algorithms. In this respect the following findings can be summarized: 1) The radar radial wind retrieval is in very good agreement with that of the profiler, considering the different nature of the scatterers involved, 2) The melting layer retrieval algorithm provides results that are in good correlation with the position of the melting layer estimated by the analysis of numerical weather prediction models, 3) Overall, QPE is satisfactory. The best results are obtained when the precipitation phase is taken into account. A small improvement is observed when Z_h-R relations are combined with A_h-R relations in the liquid phase, 4) Spectral polarimetric processing provides polarimetric variables with quality equal or better than time domain processing.

The results also show that the combination of various sensors provides a better understanding of the sensed environment.

The future work includes the analysis of hydrometeor classification algorithms and the retrieval of drop size distribution in rain by different means (spectral analysis, self-consistency, etc.). A more in-depth analysis of the events where both radars were observing simultaneously will also be performed.

ACKNOWLEDGEMENT

REFERENCES

Diederich, M., A. Ryzhkov, C. Simmer, and P. Zhang, 2015: Use of specific attenuation for rainfall measurement at X-band radar wavelengths. Part II: rainfall estimates and comparison with rain gauges. *J. Hydrometeo.,* **16,** 503-516.

Figueras i Ventura, J., A.-A. Boumahmoud, B. Fradon, P. Dupuy, and P. Tabary, 2012: Long-term monitoring of French polarimetric radar data quality and evaluation of several polarimetric quantitative precipitation estimators in ideal conditions for operational implementation at C-band. *Quart. J. Roy. Meteor. Soc.*, **138**, 2212–2228.

Figueras i Ventura, J., M. Boscacci, L. Clementi, I.V. Sideris, M. Gabella, and U. Germann, 2013: RAD4ALP, the new Swiss Doppler polarimetric weather radar network: data quality and first results. 36th AMS Conference on Radar Meteorology, Breckenridge, CO, 16-20 Sept. 2013.

Giangrande, S.E., J.M. Krause, and A.V. Ryzhkov, 2008: Automatic designation of the melting layer with a polarimetric prototype of the WSR-88D radar. *J. Atmos. Oceanic Technol,.* **47,** 1354-1364.

Gourley, J.J., A.J. Illingworth, and P. Tabary, 2009: Absolute calibration of radar reflectivity using redundancy of the polarization observations and implied constraints on drop shapes. *J. Atmos. Oceanic Technol,.* **26,** 689-703.

Moisseev, D.N., and V. Chandrasekar, 2007: Nonparametric estimation of raindrop size distributions from dual-polarization radar spectral observations, *J. Atmos. Oceanic Technol,.* **24,** 1008-1018.

_____, and _____, 2009: Polarimetric spectral filter for adaptive clutter and noise suppression, *J. Atmos. Oceanic Technol,.* **26,** 215-228.

Ryzhkov, A., M. Diederich, P. Zhang, and C. Simmer, 2014: Potential utilization of specific attenuation for rainfall estimation, mitigation of partial beam blockage, and radar networking. *J. Atmos. Oceanic Technol,.* **31,** 599-619.